water

MDPI

Article

Computational Analysis of the Kinetic Processes of Microbial Electrolysis Cell-Assisted Anaerobic Digestion Using the ADM1

Gerasimos Kanellos [1], Asimina Tremouli [1], Georgios Arvanitakis [1] and Gerasimos Lyberatos [1,2,*]

[1] School of Chemical Engineering, National Technical University of Athens, Iroon Polytechneiou 9, Zografou, 15780 Athens, Greece; gerasimoskanellos@mail.ntua.gr (G.K.); atremouli@chemeng.ntua.gr (A.T.); arvanitakis99@gmail.com (G.A.)

[2] Institute of Chemical Engineering Sciences (ICE-HT), Stadiou Str., Platani, 26504 Patras, Greece

* Correspondence: lyberatos@chemeng.ntua.gr; Tel.: +30-210-772-3256

Abstract: This study deals with the computational analysis of the kinetic processes of microbial electrolysis cell-assisted anaerobic digestion (MEC-AD) for treating raw-waste-activated sludge (WAS), compared to conventional AD, as well as investigating the effect of the organic loading rate (OLR) on the system's performance. The aim was to derive a mathematical model for the study of MEC-AD using the ADM1 framework, which can be utilized to extract the effect of an applied potential on the kinetics of AD. The experimental data were obtained from the operation of two identical reactors (an AD reactor and an MEC-AD reactor), which were operated at different OLRs. The kinetic parameters extracted from the ADM1 showed that the MEC-AD reactor yielded improved biomass yields, substrate consumption, and first-order disintegration rates, with a predominant contribution to the disintegration of complex particulates, which increased fourfold compared to the AD reactor. Moreover, it enabled operation at higher OLRs (achieving the highest divergence from the AD reactor at the OLR of 4.14 $g_{COD}/(L \times d)$), therefore accelerating WAS treatment, as well as showing an improved performance at increased solids retention time (SRT). The ADM1 exhibited efficient adaptability and predictability of the kinetic processes and can be effectively used for the optimization of the MEC-AD operation.

Keywords: ADM1; Monod substrate; hydrolysis; MEC-AD; waste-activated sludge; methanogenesis; organic loading rate

Citation: Kanellos, G.; Tremouli, A.; Arvanitakis, G.; Lyberatos, G. Computational Analysis of the Kinetic Processes of Microbial Electrolysis Cell-Assisted Anaerobic Digestion Using the ADM1. *Water* **2023**, *15*, 3939. https://doi.org/10.3390/w15223939

Academic Editors: Anastasios Zouboulis, Panagiotis G. Kougias and Konstantinos N. Kontogiannopoulos

Received: 17 October 2023
Revised: 2 November 2023
Accepted: 8 November 2023
Published: 11 November 2023

1. Introduction

Anaerobic digestion (AD) is an extensively used and accepted process, since it facilitates waste treatment, along with energy recovery, in the form of methane contained in the biogas [1]. Waste-activated sludge (WAS) is a typical AD substrate which is produced globally in large quantities, surpassing 45 million dry metric tons annually, and has a high potential for energy recovery [2,3]. However, the AD process is susceptible to limitations, which result in limited conversion of organic compounds and low methane yield. This is attributed to WAS's characteristics, specifically the nonavailability of readily biodegradable constituents of WAS, which identifies hydrolysis as the rate-limiting step in the process [4–7].

In order to overcome the challenges of AD's slow kinetics and the instabilities caused by an increase in the OLR of WAS, numerous pretreatment techniques have been proposed to enhance the biodegradability of WAS's organic components. These include mechanical, chemical, thermal, and enzymatic processes as well as combinations of them. Despite the fact that many pretreatment methods have yielded promising results, it has been reported that in many cases these methods can be energy-intensive or require the addition of chemicals, which result in ambiguous cost-effectiveness [8]. In this direction, several

innovative techniques have been recently applied in AD in order to overcome the low biodegradability issues of complex substrates, improve the energy yield of the process, and produce a higher-quality digestate. These advances include codigestion of multiple substrates, embedding biobased accelerants, or introducing a magnetic field in conventional AD, all of which have exhibited a promising effect on the stability of the process and the fertility of the digestate, and can accelerate wastewater treatment [9–12].

In this context, MEC-AD has emerged as a promising alternative to the conventional AD treatment of WAS [13–15]. Specifically, it has been found that applying a small potential in AD can result in improved waste treatment along with higher methane yield. This is achieved by the increase in the oxidation rate of nonbiodegradable organic compounds on the bioanode, while the enrichment of the microbial cultures on the biocathode (electroactive, hydrogenotrophic, and acetoclastic methanogens) facilitates the bioelectrochemical conversion of CO_2 to CH_4, which boosts methane productivity [16]. As a result, the hydrolysis of nonbiodegradable substrates is increased and the process is accelerated. Furthermore, recent studies have demonstrated that introducing accelerants or multiple substrates to be codigested in MEC-AD systems results in remarkable stability and the enhanced electrocatalytic stability of the process [17,18]. Moreover, MEC-AD energy recovery has been reported to far outperform that of conventional AD, while the energy input in the form of electricity is negligible relative to the additional methane production, resulting in high cost-effectiveness [19].

Modeling has been increasingly used for understanding the intricate actions involved in waste treatment processes, in order to ultimately design and control them. To this end, modeling of the AD process has been widely implemented, yielding important results regarding our understanding, prediction, and optimization of the complex processes taking place [20]. Anaerobic digestion model No. 1 (ADM1), developed by the International Water Association (IWA), is regarded as the most accepted and widely used model for AD [19,21]. The numerical simulation of AD can provide valuable insights and provides an effective means to optimize and regulate AD processes. ADM1 involves all AD processes, from hydrolysis to methanogenesis, as well as physicochemical dependencies and phase transition processes, in order to enable the application of the model to obtain complete mass balances [22]. Parker, 2005 [23] and Batstone and Keller, 2003 [24] summarized the application of ADM1 to advanced AD processes, and while the ADM1 processes have been extensively elaborated over the past decades, studies have recently shifted towards model simplifications, modifications, or integration with other analytical models [25–27].

However, limited research has been conducted in the field of modeling of MEC-AD's intricate processes, since this would require the integration of bioelectrochemical and abiotic redox reactions taking place on the electrodes, along with the established AD biochemical and physicochemical processes. Zou et al., 2021 [28] first developed an artificial neural network (ANN) model for an MEC-AD reactor fed with swine manure; however, the model only predicted CH_4 production, while no substrate consumption was taken into account. Nguyen et al., 2022 [29] recently developed an ANN model for the optimization of alkaline pretreated WAS-fed MEC-AD, which included both substrate consumption and CH_4 production. The results showed that at an applied potential of 0.63 V, the net energy output and monetary value of the MEC-AD reactor were optimized and significantly increased relative to conventional AD. Nevertheless, no computational studies have been performed in order to describe the raw-WAS-fed MEC-AD reactor, to extract the kinetic parameters of the MEC-AD along with delineation of the effect that the applied potential has on the kinetic processes, or to identify the effect that the OLR has on raw WAS treatment.

In this context, the purpose of the current study is to render the raw-WAS-fed MEC-AD process foreseeable and predictable by using the ADM1 framework. Experimental data obtained from the long-term operation of two identical reactors, one used as a conventional AD reactor and the other as an MEC-AD reactor, were used for the present study. The aim was to derive a single kinetic and mathematical model for the study of the AD reactor

in comparison with the MEC-AD reactor. This custom model can therefore serve as a guide showing the quantitative difference that the effect of an applied potential has on the Monod-type and on the first-order kinetics of AD, which involve substrate consumption, disintegration of particulates, hydrolysis, and biomass concentrations. ADM1 extracts the kinetic parameters for the AD reactor biochemical processes, while in the case of the MEC-AD reactor, the bioelectrochemical interactions and redox reactions taking place on the electrodes are not taken into consideration. It can therefore serve as an imprint of the quantitative effect that an MEC-AD would have on the kinetics of its biochemical processes, in comparison with a conventional AD. This is the first study that addresses the efficiency, adaptability, and predictability of the ADM1 framework in optimizing MEC-AD's operation.

2. Materials and Methods

2.1. Experimental Setup and Operation

The experimental raw-WAS-fed AD's and MEC-AD's datasets were obtained from Kanellos et al., 2024 [30], in order to extract the kinetic parameters of each process using the ADM1. As shown in Figure 1, two identical 2 L reactors were constructed and operated as an AD and an MEC-AD reactor. The reactors were cylindrical glass vessels and were equipped with an inlet/outlet tube in order to facilitate the draw–fill operation mode. Additionally, a biogas outlet was incorporated at the top of each reactor, connected to a biogas sampling port and a U-shaped oil displacement technique that was recorded by an electro-optic level switch and a programmable logic controller (PLC) to record the biogas production. Two carbon felt electrodes (each with an area of 25 cm^2) were submerged in the MEC-AD reactor and were connected with an external power supply through titanium wires in order to control the applied potential. A constant voltage of 1 V was applied between the carbon felt electrodes in a two-electrode configuration. The applied voltage of 1 V was chosen as a reasoned value within the range of potentials (0.3–2 V) that have been employed in other studies, aiming to optimize the MEC-AD process in terms of substrate degradability and obtained methane yields [31–34].

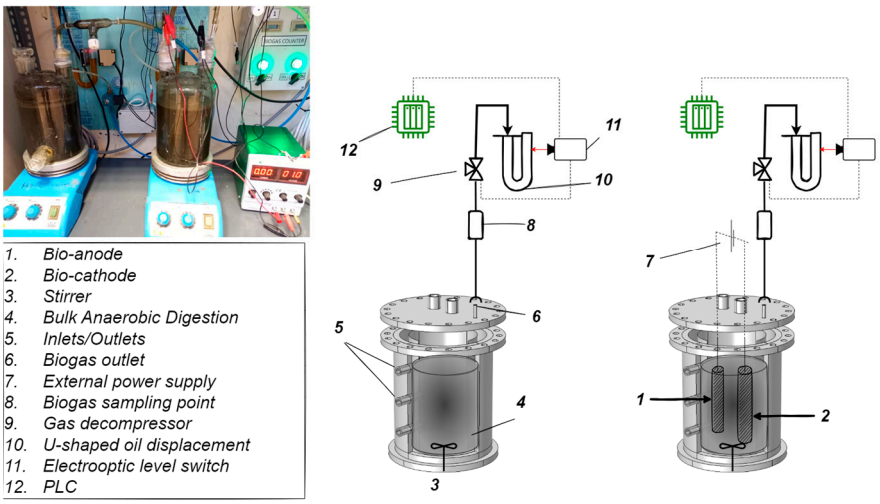

Figure 1. The schematic diagram of the AD and MEC-AD reactors.

The reactors were operated at a constant temperature of 30 °C and were constantly stirred through magnetic stirring. The raw WAS was obtained from the Municipal Wastewater Treatment Plant of Lykovrisi, in Attica, Greece, and its characteristics are presented in Table 1. The reactors were operated for a total of 131 days with the raw WAS at different organic loading rates (OLRs) of 1.1, 1.7, and 2.9 $g_{COD}/(L \times d)$.

Table 1. The physicochemical characterization of the raw WAS used during the operation of the reactors.

Parameter	Units	Value
pH	-	6.8
Total alkalinity	$gCaCO_3/L$	4
Conductivity	mS/cm	1.5
Total solids	g/L	22
Volatile solids	g/L	16
Total suspended solids	g/L	21
Volatile suspended solids	g/L	15
Soluble COD	gO_2/L	0.5–1
Total COD	gO_2/L	25
Acetic acid	mg/L	110
Propionic acid	mg/L	75
Iso-butyric acid	mg/L	21
Butyric acid	mg/L	15
Iso-valeric acid	mg/L	10
Valeric acid	mg/L	2
Ethanol	mg/L	180
Total Kjeldahl nitrogen	g_N/L	1.25
Particulate organic carbon	g_C/L	8.5

2.2. Model Description

The modeling of the reactors' operation was performed using the Aquasim 2.0 software and the mathematical model ADM1. ADM1 includes the five stages of AD (degradation, hydrolysis, acidogenesis, acetogenesis, and methanogenesis) along with the action of biological enzymes at each stage. The processes simulated in the model are divided into biochemical and physicochemical. Biochemical processes are catalyzed by enzymes that act intracellularly or extracellularly and are considered irreversible. In contrast, physicochemical processes involve ion exchange (acid/base balance) and liquid/gas transfer phenomena (liquid/gas phase equilibrium) and are considered reversible reactions [24].

The model contains 26 variables which are required to fully define the system at a given point. Among them, 12 refer to soluble components: monosaccharides, amino acids, long-chain fatty acids (LCFAs), total volatile fatty acids (VFAs), hydrogen, methane, inorganic carbon (dissolved CO_2), inorganic nitrogen (dissolved ammonia), and soluble inerts. In addition, 5 variables refer to suspended particles in the reactor: complex particulates, carbohydrates, proteins, lipids, and particulate inerts. An additional 2 variables serve to describe the acid/base balance of the described system; anion and cation concentrations. Finally, 7 important variables for the model are those of biomass concentrations. Specifically, for each soluble substrate (LCFAs, amino acids, sugars, valeric acid, butyric acid, propionic acid, acetic acid, and hydrogen), the model considers a respective type of biomass that metabolizes it (except for methane, which is the final product) [35]. Intracellular biochemical reactions involving substrate consumption follow Monod-type kinetics. In contrast, disintegration of particulates, hydrolysis (extracellular reactions), and biomass death are represented by first-order kinetics. Dead biomass is retained in the system and is a composite particulate material that acts as a substrate that is gradually degraded. Inhibitory effects shown in ADM1 include pH (affects the action and growth of all microorganisms), hydrogen (affects homoacetogenic bacteria, which facilitate the acetate production by reducing

CO_2 along with molecular H_2), and free ammonia (affects acetoclastic methanogens, which facilitate the methane production through acetate oxidation) [24].

The ADM1 model was developed and adapted to the experimental data of both reactors during all operating phases in a continuous mode to simulate the draw–fill operation. The modeling of the reactors was based on the carbon and nitrogen balance between solids decomposition and biogas production. During the simulation, the experimental data entered in the model for the feed as well as for both bioreactors were the reactor volume, the inlet supply rate, the soluble chemical oxygen demand (sCOD) and total chemical oxygen demand (tCOD), the soluble and particulate carbon, the soluble and particulate nitrogen, and the total and volatile (suspended) solids (TS, VS, TSS, and VSS).

2.3. Model Setup and Equations

As the ADM1 includes multiple kinetic parameters that have a certain impact on the process and the final products, certain assumptions were made in order to calibrate the model before the parameter estimation and the sensitivity analysis. The simplified assumptions can be summarized as follows: the disintegration of dead biomass follows the same first-order kinetics as the rest of the complex particulates; all microorganisms decay following first-order kinetics with a decay coefficient of $k_{dec} = 0.02\ d^{-1}$; the complex particulates disintegrate towards constant fractions of carbohydrates ($f_{ch} = 0.2$), lipids ($f_{li} = 0.35$), proteins ($f_{pr} = 0.2$), and particulate inerts ($f_{in} = 0.25$), as suggested by Batstone and Keller, 2003 [24] (p. 46, Table 6.1); fractions of amino acids and sugars towards VFAs and H_2, as well as yields of biomass (Y_i—$kgCOD_X\ kgCOD_S{}^{-1}$) on uptake of soluble substrates, are considered constant, as suggested by Batstone and Keller, 2003 [24] (p. 46, Table 6.1); the pH is set as constant and equal to 7 based on the experimental behavior of the reactors, so no inhibitory actions are considered due to pH variations in the substrate uptake processes; the uptake rates of butyrate and valerate are identical and metabolized by the same microorganisms [36]; the solids retention time (SRT) is initially considered equal to the hydraulic retention time (HRT), as the experimental reactors described by ADM1 are continuously stirred.

The complete ADM1 algorithm for the biological kinetic rate expressions and coefficients is employed as initially described by Henze et al., 1986 [37] (pp. 506–507, Table 1). In order to extract the functions of the degree of influence of the kinetic constants on the soluble and particulate organic load, ADM1 varies each constant, one at a time, by a small percentage (typically 1%), and the differences from the original calculation is used to establish a new balance on the system. Due to the constant pH applied in ADM1, no empirical inhibition expressions were employed, which are a direct consequence of high or low pH in the reactors. Instead, noncompetitive inhibition, caused by hydrogen and free ammonia inhibition, as well as substrate limitation inhibition, caused by total ammonia limitation, are considered in the model [24,38].

3. Results and Discussion

3.1. Model Results and Validation

3.1.1. ADM1 Fit to the Experimental Data

The target variables which were selected for simulation using the ADM1 included the reactors' COD, carbon and nitrogen content, in both their particulate and soluble form, along with the produced biogas and its methane content. Figures 2–5 present the experimental and simulated values of the aforementioned parameters, following the carbon and nitrogen mass balances of the reactors.

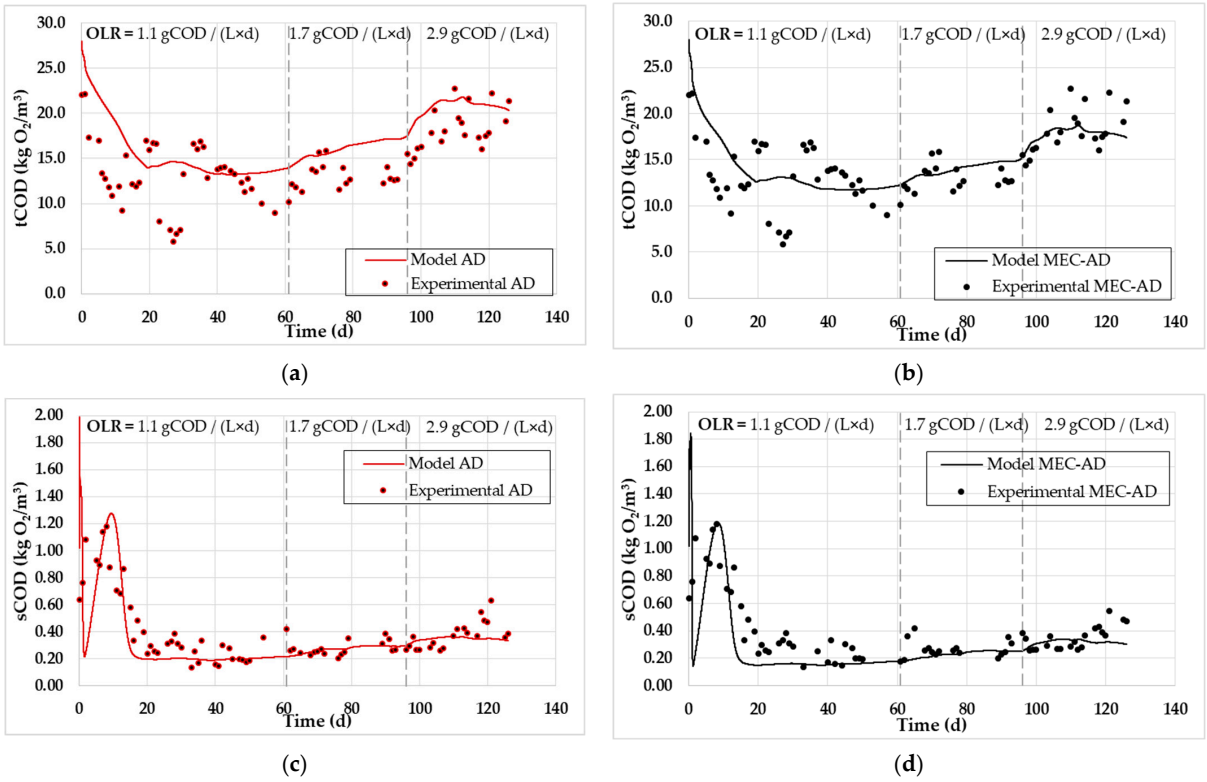

Figure 2. The experimental values (symbol) and the computational fit (line) of (**a**) tCOD of the AD reactor, (**b**) tCOD of the MEC-AD reactor, (**c**) sCOD of the AD reactor, and (**d**) sCOD of the MEC-AD reactor, as was obtained from ADM1.

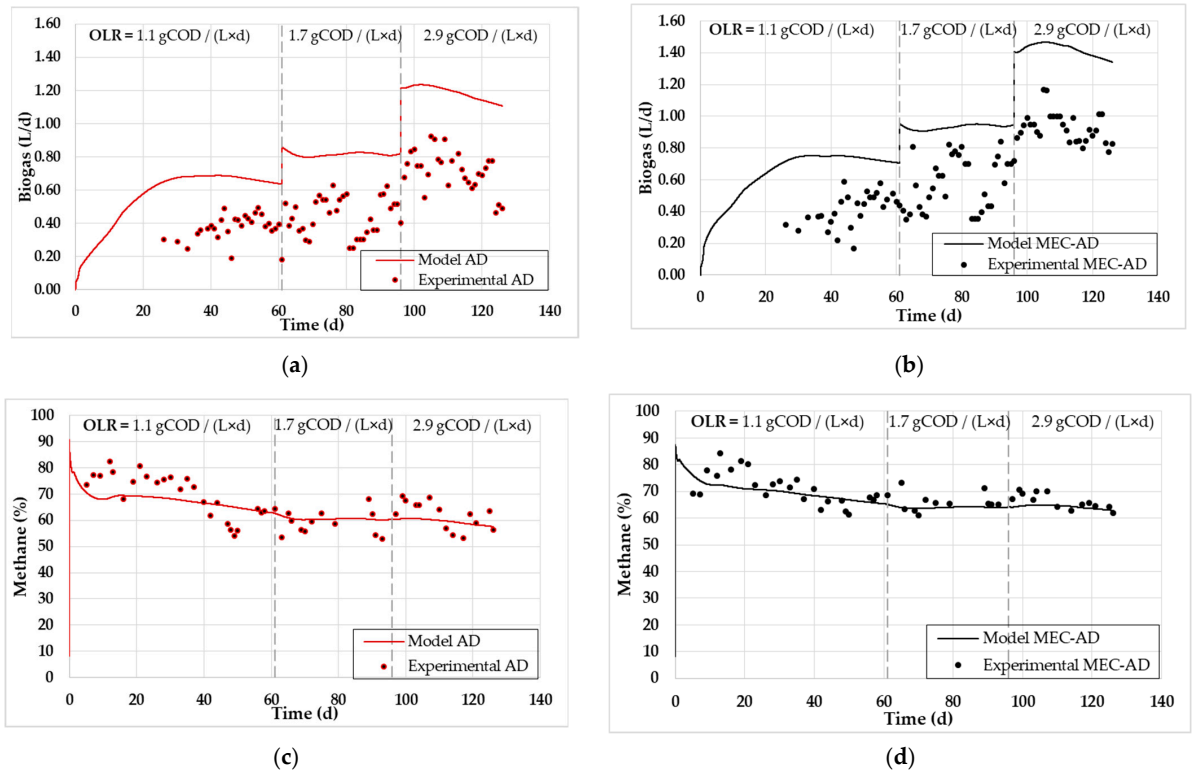

Figure 3. The experimental values (symbol) and the computational fit (line) of (**a**) biogas of the AD reactor, (**b**) biogas of the MEC-AD reactor, (**c**) methane content of the AD reactor, and (**d**) methane content of the MEC-AD reactor, as was obtained from ADM1.

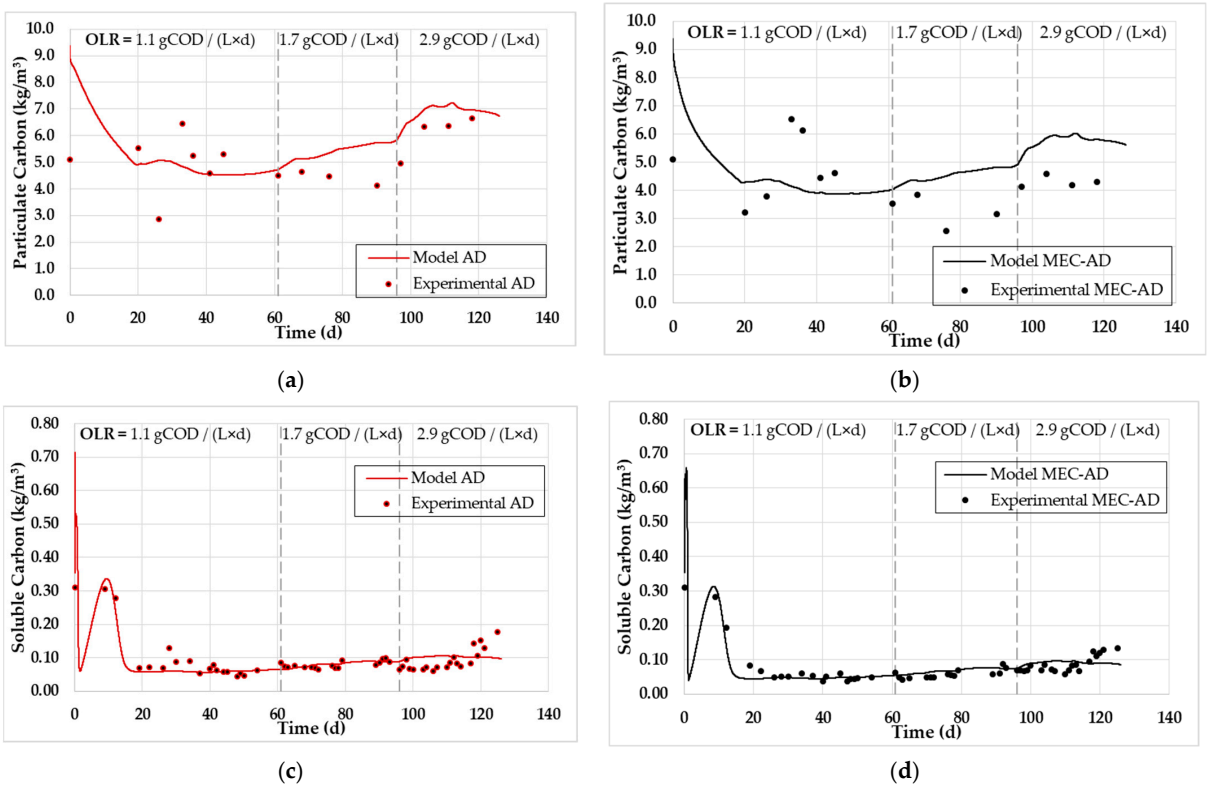

Figure 4. The experimental values (symbol) and the computational fit (line) of (**a**) particulate carbon of the AD reactor, (**b**) particulate carbon of the MEC-AD reactor, (**c**) soluble carbon of the AD reactor, and (**d**) soluble carbon of the MEC-AD reactor, as was obtained from ADM1.

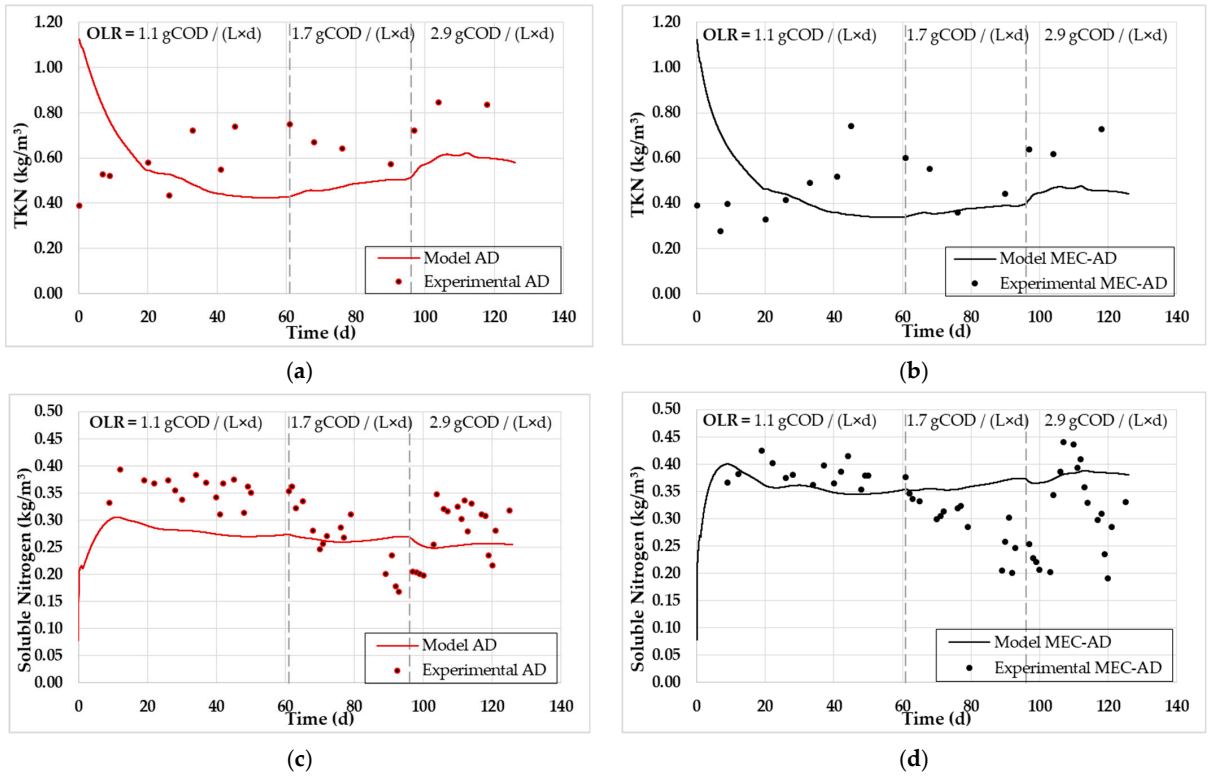

Figure 5. The experimental values (symbol) and the computational fit (line) of (**a**) TKN of the AD reactor, (**b**) TKN of the MEC-AD reactor, (**c**) soluble nitrogen of the AD reactor, and (**d**) soluble nitrogen of the MEC-AD reactor, as was obtained from ADM1.

The analysis showed an adequate fit of the variables studied for both reactors. Specifically, the values of particulate (Figure 4a,b) and soluble carbon (Figure 4c,d), as well as those of soluble COD (Figure 2c,d), soluble nitrogen (Figure 5c,d), and methane content (Figure 3c,d), achieved the best fit, while some deviation was observed for the fitting of tCOD (Figure 2a,b) and TKN (Figure 5a,b), which were slightly overrated (by 2 g/L) and devalued (by 0.2 g/L), respectively. Accordingly, this deviation in the particulate parameters (tCOD and TKN) resulted in an equivalent deviation in the simulated produced biogas in both reactors (Figure 3a,b), which was slightly overestimated by approximately 0.5 L/d. The deviation of tCOD can be explained by the presence of oxidizable inorganic compounds in the raw WAS, which are not taken into account by ADM1, while the deviation of TKN could be attributed to the fact that the content of amino acids in the raw WAS were not measured, but were instead considered based on an average WAS composition. These deviations appear to be marginally increasing as a function of the increase in OLR (from 1.1 to 2.9 $g_{COD}/(L \times d)$), especially for the case of the AD reactor, which can be attributed to the fact that a less efficient AD process occurs at high OLRs, as has been previously observed [30].

Moreover, comparing the curves predicted by the model for both cases, the AD reactor generates higher values for particulate carbon, tCOD, and TKN content (Figures 2a, 4a and 5a, respectively), in comparison with the MEC-AD reactor (Figure 2b, Figure 4b, and Figure 5b, respectively) for all OLRs examined, which is also the case with the experimental values. In addition, the generated values of soluble carbon, sCOD, and soluble nitrogen (Figures 2d, 4d and 5d, respectively) appear slightly increased in the MEC-AD reactor simulation, which is a direct consequence of the increased decomposition of particulate matter and their hydrolysis towards their soluble forms. The results are in accordance with previous studies that have focused on the effect of the applied potential on the enhancement of the hydrolysis step in anaerobic digestion [4,5,15,30]. Furthermore, Figure 6 depicts the predicted biomass concentrations in both reactors, where the simulation predicts that the MEC-AD reactor yields marginally increased cumulative biomass concentrations. This divergence became more apparent at high OLRs and reached a maximum divergence of ~0.4 g/L (Figure 6c).

Overall, the MEC-AD reactor exhibits a higher hydrolysis rate of particulate compounds (tCOD, carbon, and nitrogen) towards their soluble forms and this is accurately depicted through the ADM1 (Figures 2–5). The increased hydrolysis rate can be attributed to both the enrichment of the microbial consortia present in the MEC-AD reactor and their activity. Specifically, apart from the quantitative increase of the microbes in the MEC-AD reactor (Figure 6), their variety is also larger, as additional exo- and endoelectrogens are developed in the integrated system [39]. In addition, when an appropriately high voltage is applied, the bacteria metabolism can be improved and the cell rupture rate can be decreased on both the anodic and the cathodic biofilms [16]. Moreover, the soluble compounds (sCOD, carbon, nitrogen) produced from the hydrolysis step do not present significant accumulation in the MEC-AD reactor, relative to the AD reactor, as they are fitted in a similar concentration range. It has been shown that conductive carbon materials, such as the carbon felt employed in the current study, can enhance the process efficiency by providing more active sites, which can facilitate localized substrate accumulation. As a result, the mechanism that underlies the higher efficiency of the MEC-AD reactor, in terms of increased substrate oxidation and methane yield, is attributed to the increased direct interspecies electron transfer (DIET) and the better ion migration in the electrolyte/electrode interfaces [17,40].

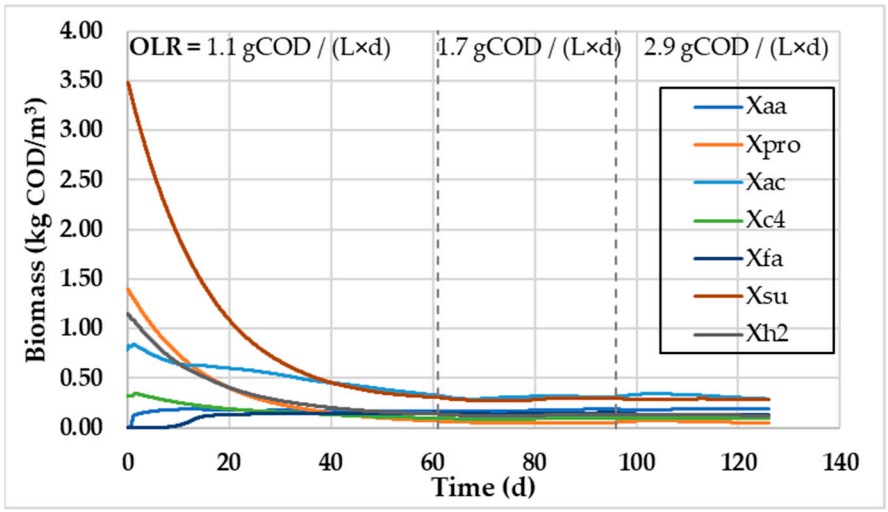

(**a**)

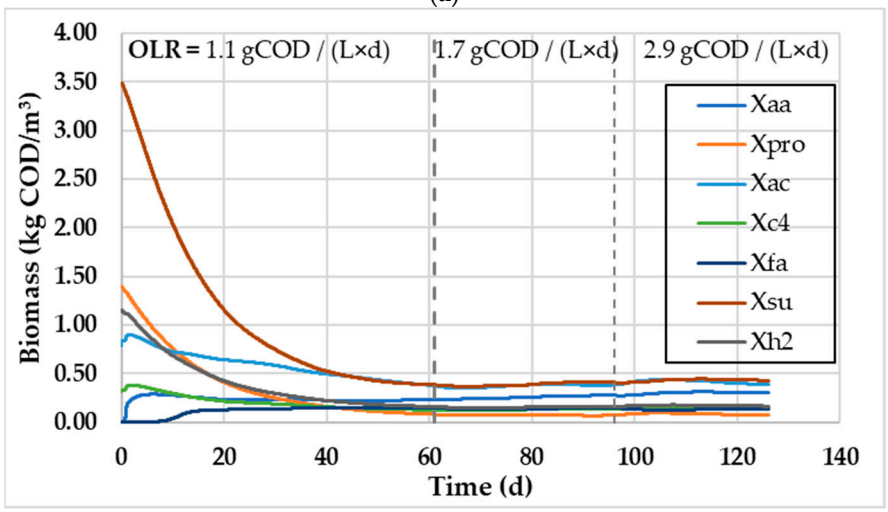

(**b**)

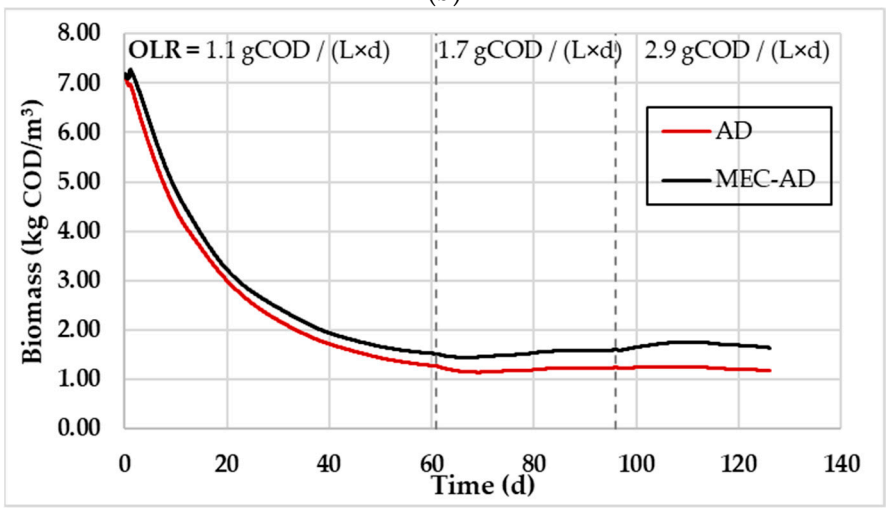

(**c**)

Figure 6. The simulated individual biomass (X—kgCOD$_X$ m^{-3}) concentrations (where aa is amino acids; ac is acetate; c4 is butyrates; fa is fatty acids; h2 is hydrogen; pro is propionate; su is sugars) in the (**a**) AD reactor and (**b**) MEC-AD reactor, and (**c**) the cumulative biomass concentration in the reactors, as was obtained from ADM1.

3.1.2. Estimation of Kinetic Parameters

Accordingly, the estimated parameters from the computational fitting were the Monod kinetic constants (k_m and K_s) for all soluble substrates, as well as the first-order kinetic constants for the disintegration of complex particulates and for the hydrolysis of carbohydrates, proteins, and lipids to sugars, amino acids, and LCFAs, respectively. Table 2 shows the deduced kinetic values for both reactors, while the Monod reaction rates are depicted in Figure 7.

The performed parameter estimation resulted in better kinetic processes for the MEC-AD reactor, which agrees with the faster hydrolysis of particulate matter presented in Figures 2–5. The obtained values for the Monod and first-order disintegration kinetic constants were estimated by utilizing upper and lower value limits, which were set independently for each parameter, as has been previously described [24] (p. 47, Table 6.2). Specifically, the vast majority of the Monod kinetic constants (k_m and K_s), which describe the substrate uptake rate, were noticeably enhanced, resulting in both higher k_m and lower K_s values for each substrate. The uptake rates of amino acids (Figure 7a), LCFAs (Figure 7c), acetate (Figure 7e), and the butyrate and valerate (Figure 7g) are considerably enhanced in the case of the MEC-AD reactor. Moreover, the uptake rate of sugars (Figure 7b) converges at very high concentration values, whereas the uptake rate of propionate (Figure 7f) appears faster for the MEC-AD reactor at low concentrations and slightly higher for the AD reactor in very high concentrations. Despite the faster substrate uptake rate in the majority of the MEC-AD reactor variables, the H_2 consumption is much faster in the AD reactor (Figure 7d), which, however, does not compensate for the higher uptake rate of amino acids, sugars, LCFAs, and VFAs in the MEC-AD reactor. These are the same parameters that are considered to be limiting factors for the AD process [14], while the lower H_2 consumption of the MEC-AD reactor could be attributed to intermediate redox reactions that utilize H_2, such as the indirect electromethanosynthesis or the abiotic H_2 production, which take place on the biocathode and are not considered in the present model [41]. Nevertheless, the H_2 concentration is considered in the ADM1 mass balances, which results in higher predicted biogas production and CH_4 content (Figure 3). In addition, the deduced values could be interpreted as higher substrate-to-biomass and substrate-to-energy yields in the MEC-AD reactor, which may be attributed to the fact that the same amount of metabolized substrate results in more biomass and energy production, respectively, and, therefore, more metabolic products and ultimately more methane. Furthermore, the MEC-AD reactor showed similar first-order hydrolysis kinetic constants for the decomposition of carbohydrates, lipids, and proteins to that of the AD reactor (Table 2), while a noticeable difference was obtained for the disintegration of complex particulates (0.4 g/L for the MEC-AD reactor and 0.1 g/L for the AD reactor). As a result, ADM1 perceives the faster disintegration of complex particulates to be the most crucial parameter for the fitting to the experimental values, which are distinguished by the potential application in the MEC-AD reactor.

The obtained results demonstrate the extent of the improvement of the MEC-AD reactor kinetic parameters (Monod uptake and first-order disintegration) relative to the AD reactor during raw-WAS treatment. The enhancement of the MEC-AD reactor kinetic parameters is attributed to the presence of the electrodes. Specifically, the carbon felt provides large porosity and increased active sites, which enable the attachment, growth, and extracellular electron transfer of the bacteria [28]. Moreover, the applied potential provides the activation energy for the oxidation of some organic substrates and the bioelectrochemical reduction of CO_2 to CH_4. Combined with the fact that both the quantity and variety of the microorganisms are enriched, the reduction of particulate and soluble substrates is accelerated and the stability of the process is promoted.

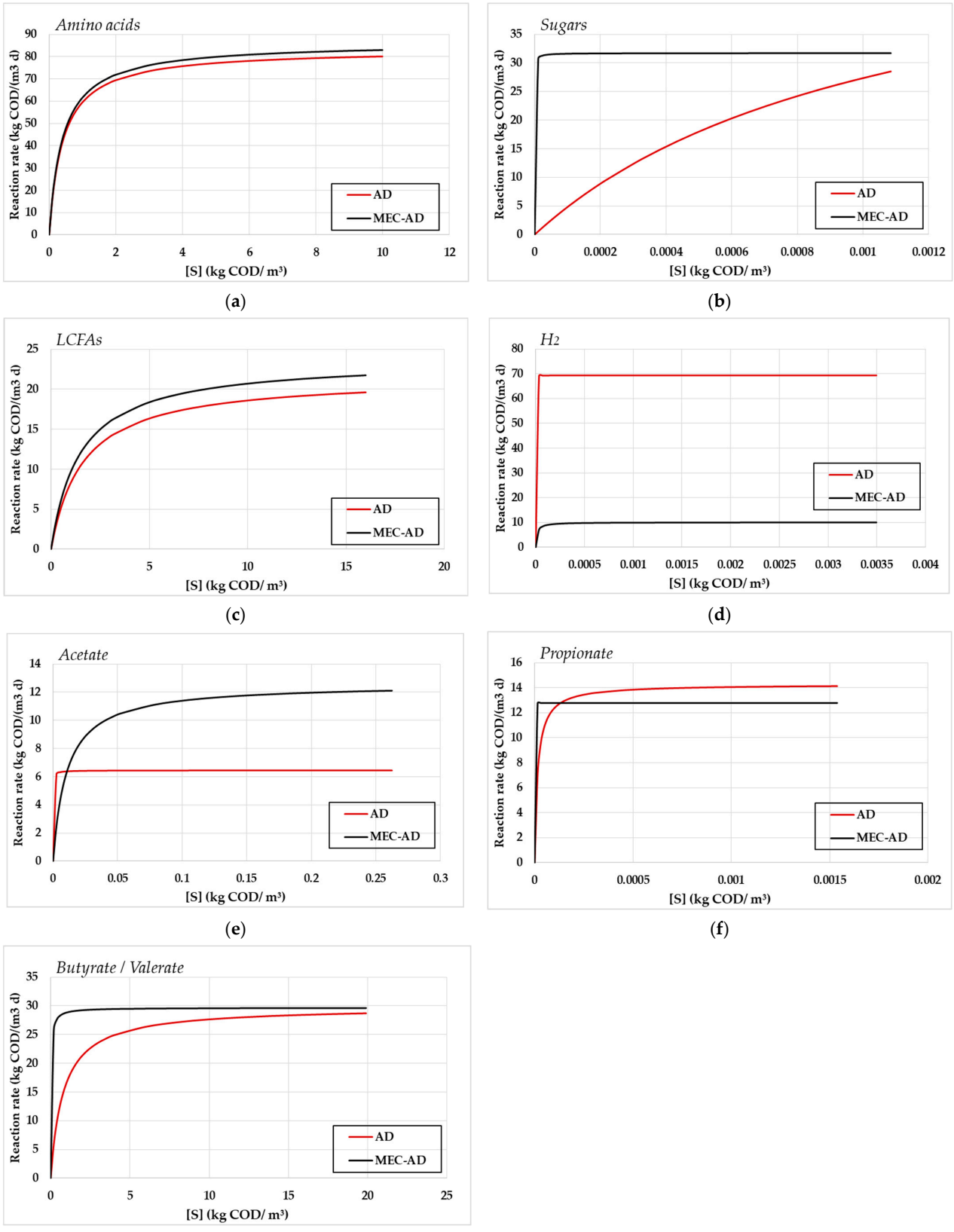

Figure 7. The substrates' (S—kgCOD$_S$ m^{-3}) uptake Monod kinetic rate of (**a**) amino acids, (**b**) sugars, (**c**) LCFAs, (**d**) H_2, (**e**) acetate, (**f**) propionate, and (**g**) butyrate/valerate for the AD reactor (red) and the MEC-AD reactor (black) as a function of each substrate concentration.

Table 2. The substrates' uptake Monod kinetic constants and the particulates disintegration and hydrolysis first-order kinetic constants as they occur from the fitting of ADM1 to the experimental values.

Substrate Uptake Monod Kinetic Constants					**Disintegration First-Order Kinetic Constants**		
	AD		**MEC-AD**			**AD**	**MEC-AD**
	$\mathbf{k_m}$ **(kgCOD$_S$ kgCOD$_X$ d^{-1})**	$\mathbf{K_s}$ **(kgCOD$_S$ m^{-3})**	$\mathbf{k_m}$ **(kgCOD$_S$ kgCOD$_X$ d^{-1})**	$\mathbf{K_s}$ **(kgCOD$_S$ m^{-3})**		**(d^{-1})**	**(d^{-1})**
Amino acids	83.3	0.4	86.3	0.4	Carbohydrates	19.9	19.9
Sugars	57.1	1.1×10^{-3}	31.7	3.3×10^{-7}	Lipids	0.1	0.1
LCFAs	21.6	1.6	23.7	1.5	Proteins	39.9	39.5
H_2	69.3	6.7×10^{-8}	10.1	1.4×10^{-5}	Particulates	0.1	0.4
Acetate	6.4	1.1×10^{-4}	12.6	1.1×10^{-2}			
Propionate	24.3	1.5×10^{-5}	12.8	5.5×10^{-9}			
Butyrate/Valerate	29.9	7.9×10^{-1}	29.7	2.9×10^{-2}			

3.1.3. Sensitivity Analysis of Kinetic Parameters

Figure 8 shows the sensitivity analysis for all kinetic parameters (Monod and first-order disintegration constants), and the effect their variation causes on the sCOD and the tCOD content of the reactors.

In general, higher values of each parameter function result in larger changes in the calculated variables following the small change in the kinetic constants, which means that the system is more susceptible to the respective change and has a greater sensitivity to each kinetic constant. The spikes of some kinetic parameters, presented in Figure 8a–e, are attributed to the changes in OLR values and appear to stabilize within a few days after the reactors have reached a new steady state. Regarding the sCOD consumption, the Monod and the first-order kinetic constants have a marginally increasing sensitivity as a function of increasing OLR. However, the sCOD consumption shows the highest sensitivity to the LCFAs uptake, which is a major limiting factor in AD, while the uptake of other substrates influences the processes to a lesser extent (Figure 8a–d). The results indicate that the disintegration of complex particulates is the most sensitive parameter to changes, resulting in the highest variations of tCOD decomposition (Figure 8f). Moreover, the first-order hydrolysis constant of lipids shows some sensitivity to changes, while the hydrolysis of proteins and carbohydrates does not significantly affect the processes (Figure 8f).

3.2. Optimization of Raw-WAS-Fed MEC-AD by the ADM1

3.2.1. Organic Loading Rate

The obtained kinetic parameters from the ADM1 fit to the experimental data were utilized in order to extract the predicted tCOD consumption and accumulation in the reactors, in relation to varying OLR (from 1.2 to 12.4 $g_{COD}/(L \times d)$). Figure 9 depicts the results from the predicted differences between the two reactors.

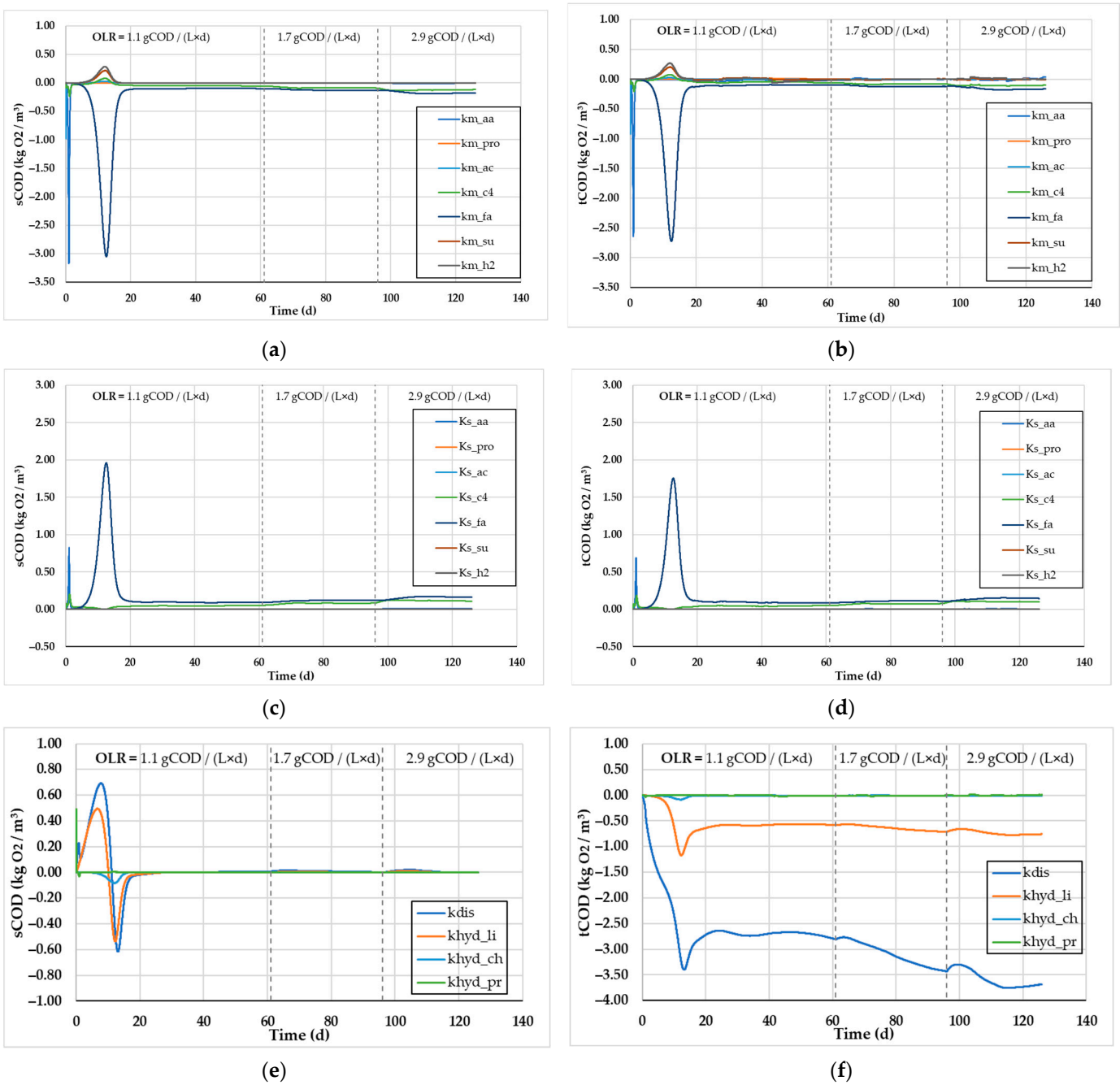

Figure 8. The sensitivity analysis of (**a**) sCOD and (**b**) tCOD as a function of the k_m Monod; the sensitivity analysis of (**c**) sCOD and (**d**) tCOD as a function of the K_s Monod; and the sensitivity analysis of (**e**) sCOD and (**f**) tCOD as a function of the first-order disintegration kinetic constants (where aa is amino acids; ac is acetate; c4 is butyrates; fa is fatty acids; h2 is hydrogen; pro is propionate; su is sugars; dis is for complex particulates; li is for lipids; ch is for carbohydrates; pr is for proteins), as was obtained from ADM1.

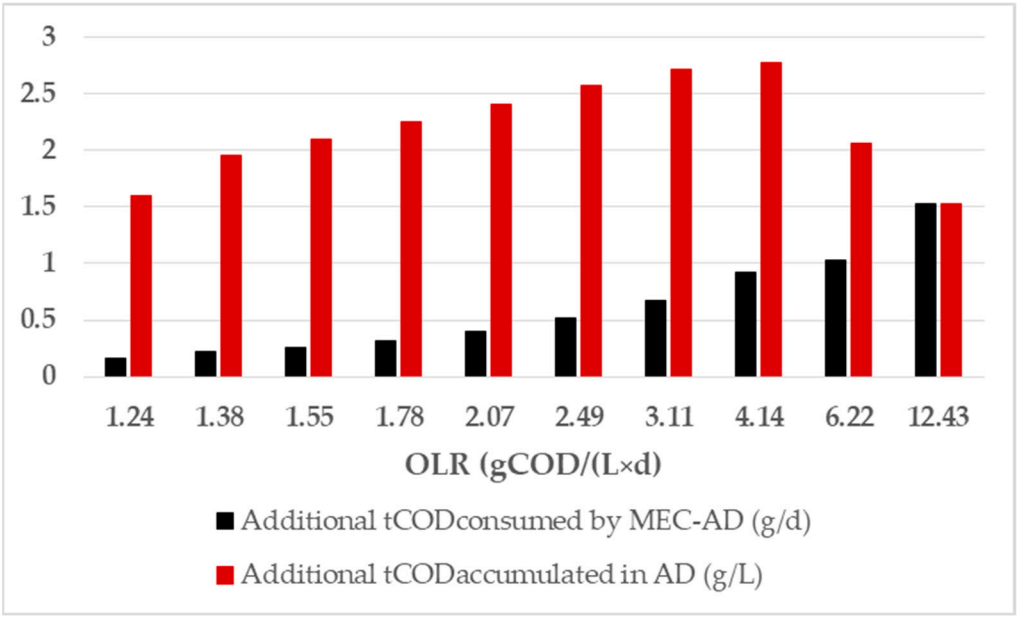

Figure 9. The simulated divergence in the MEC-AD reactor consumed tCOD (black) and the AD reactor additional accumulated tCOD relative to the MEC-AD reactor (red) in relation to the reactors OLR, as was obtained from ADM1.

As shown in Figure 9, ADM1 predicts a linearly increasing additional consumption in the MEC-AD reactor (from 0.2 to 1.5 g_{COD}/d), relative to the AD reactor, as a function of increasing OLR (from 1.2 to 12.4 $g_{COD}/(L \times d)$). This result is a direct consequence of the higher disintegration rate of complex particulates (Table 2). Furthermore, the comparative prediction shows that the MEC-AD reactor exhibits the highest divergence from the AD reactor, at the OLR of 4.14 $g_{COD}/(L \times d)$, where the additional COD consumption rate of the MEC-AD reactor, relative to the AD reactor, is 0.9 g_{COD}/d. At that OLR, the accumulated COD in the AD reactor presents a maximum concentration (accumulation rate of 2.7 g_{COD}/d in addition to that of the MEC-AD reactor), while further increase in the OLR results in a simulated deterioration of both processes. These results are in accordance with previous findings indicating that the applied potential exploitation is enhanced at relatively high OLR values and therefore high substrate availability [30,42,43]. Moreover, the operation of the reactors at very high OLRs (>6.22 $g_{COD}/(L \times d)$) and mesophilic conditions results in the deterioration and instability of the processes, as a drop in alkalinity and accumulation of VFAs can occur [44]. Although the OLR has no significant effect on the AD kinetic processes, it is a crucial parameter that has to be optimized based on the kinetic processes of the MEC-AD system. In particular, as shown in Figure 9, while the MEC-AD reactor can greatly increase the additional tCOD consumption at very high OLRs (additional consumption rate of up to 1.5 g_{COD}/d relative to the AD reactor), the optimal operation (and therefore the best energy utilization and digestate quality) is predicted at an OLR of 4.14 $g_{COD}/(L \times d)$. The results indicate that the optimization can significantly improve the treatment performance and economic efficiency of the raw-WAS-fed MEC-AD reactor as it achieves faster treatment times and better effluent quality relative to the AD reactor.

The MEC-AD is a multifactorial process that depends on the cell layout, the electrode materials, the substrate employed, and the operating conditions (temperature, OLR, applied potential, SRT). Limited studies have been conducted on the effect of OLR during raw WAS treatment in mesophilic MEC-AD systems. Specifically, it has been shown that the optimal MEC-AD operation under thermophilic conditions was obtained at an OLR of 18 $g_{COD}/(L \times d)$ [43]. In addition, an MEC-AD studied under psychrophilic conditions

could overcome the process deterioration presented by an increased OLR of 4.5 $g_{COD}/(L \times d)$; however, amendment with granular activated carbon was employed [42].

Another crucial parameter that affects the treatment efficiency and methane yield is the applied potential. For this purpose, a wide range of potentials have been studied (0.3–2 V) which have yielded dissimilar results in terms of optimal operation [30]. This is mostly attributed to the differences in the MEC-AD systems, as previously stated. In this context, while the minimum theoretical applied voltage for MEC-AD systems is 0.14 V, this can lead to inefficient substrate degradability or biogas upgrading. The optimal applied voltage in several studies that have examined this effect is found to be in the range of 0.5–0.9 V; however, the cell layouts and operating conditions greatly vary [18,31,45,46]. Among four different models studied for a swine-manure-fed MEC-AD system, the ANN model was superior and yielded the optimal methane yield at the applied potential of 0.9 V, while no optimization of the OLR took place [28]. Moreover, the ANN model developed for the optimization of the applied potential in an alkaline pretreated WAS-fed MEC-AD system was optimized at the value of 0.63 V; however, the effect of the OLR was not taken into consideration [29]. On the other hand, it has been reported that high voltages ($\geq$1 V) can improve AD by creating microaerobic conditions through in situ electrolytic oxygen, which can lead to enhanced methane yield, while very high applied voltage ($\geq$1.6 V) resulted in inhibition of methane yield by causing microbial damage and lowering the microbial activity [34].

3.2.2. Solids Retention Time

As has been previously described, the SRT of a reactor is a crucial parameter for its operation, as it directly affects the stability and activity of the microbial populations involved in the digestion process [46]. Moreover, taking into consideration that the SRT is equal to the HRT during ideal reactor mixing, it stands to reason that the SRT deviates from the HRT since some biomass can be withheld in the reactor. As a result, further optimization of the kinetic parameters took place by simulating the MEC-AD's operation at an increased SRT, which was set equal to the HRT plus 1.5 d.

The results for the predicted values of the kinetic parameters are presented in Table 3. These show that the majority of the kinetic parameters appeared to be improved relative to the corresponding values at lower SRTs (Table 2). Specifically, the majority of k_m values (for amino acids, sugars, LCFAs, and all VFAs) increased, indicating a faster maximum uptake of each corresponding substrate, as a higher biomass concentration was present in the MEC-AD reactor. The exception to this is the k_m value for H_2 uptake, which appeared to be slightly decreased relative to that at a lower SRT (Table 2). The fact that H_2 uptake was further reduced as a function of increased SRT infers that the increased biomass concentration resulted in higher inhibition. This is due to the mass balances used by ADM1 in order to extract the fit to the experimental data (Figures 2–5) and could be attributed to the limited concentration of homoacetogenic bacteria, which utilize molecular H_2 towards CH_4 production. Moreover, the increase of the SRT appears to have mixed effects on the saturation constants (K_s) for each substrate, as the K_s values for the sugars and propionate were improved, those for H_2, acetate, and butyrate/valerate were deteriorated, and the values for amino acids and LCFAs remained practically constant. Despite these changes, which were also shown to have a limited sensitivity to the reactor operation (Figure 8a–d), the overall Monod substrate uptake kinetics were better as a function of increased SRT. Furthermore, the first-order disintegration constants also showed mixed results, with a slightly decreased carbohydrate disintegration, a constant disintegration of lipids, and improved disintegration of proteins and complex particulates. Specifically, the disintegration of complex particulates, which was found to be the most sensitive parameter to changes (Figure 8f) and the main cause of variation between the AD and the MEC-AD reactors, increased drastically (0.7 g/L relative to 0.4 g/L for high and low SRTs, respectively). Overall, the first-order disintegration constants, similarly to the Monod constants, contributed towards an improved process at higher SRTs.

Table 3. The substrates' uptake Monod kinetic constants and the particulates disintegration and hydrolysis first-order kinetic constants as they occurred from the fitting of ADM1 to the experimental values of the MEC-AD reactor at an increased SRT.

Substrate Uptake Monod Kinetic Constants			**Disintegration First-Order Kinetic Constants**	
	MEC-AD			**MEC-AD**
	$\mathbf{k_m}$ **(kgCOD$_S$ kgCOD$_X$ d^{-1})**	$\mathbf{K_s}$ **(kgCOD$_S$ m^{-3})**	**(d^{-1})**	**(d^{-1})**
Amino acids	95.2	0.4	Carbohydrates	19.8
Sugars	51.2	4.7×10^{-3}	Lipids	0.1
LCFAs	23.7	1.5	Proteins	31.7
H_2	8.7	1.1×10^{-5}	Particulates	0.7
Acetate	13.6	4.6×10^{-4}		
Propionate	23.3	9.1×10^{-4}		
Butyrate/Valerate	37.6	0.2		

An effective way to significantly vary the SRT from the HRT is to incorporate recycling in the reactor. Effluent recycling can prove advantageous in the treatment efficiency and operation time of the process, as it enables increased SRTs that lead to faster WAS treatment without significant washout of methanogenic bacteria, which have the highest generation time relative to all other microorganisms [47]. In addition to the faster treatment time and the higher efficiency (Table 3), the digestate quality is improved. In this context, the digestate can have increased upcycling potential in order to completely utilize the WAS resource. The effect of carbon biobased materials on the increased stability and fertilizability of the digestate has been previously addressed [40]. Moreover, the MEC-AD process could potentially be coupled with low-cost composited accelerants or salt additives, which can lead to further improvements to the digestate quality, such as increased trace elements, nutrients content, and fertility, therefore increasing the waste biomass utilization potential [48,49].

4. Conclusions

The present study assessed the ADM1 framework efficiency, adaptability, and predictability in extracting the kinetic processes of a raw-WAS-fed MEC-AD reactor in comparison with an AD reactor. In addition, ADM1 was effectively used for the optimization of the apparent Monod and first-order kinetic constants of the MEC-AD reactor. For this purpose, the experimental dataset of two identical reactors (an AD reactor and an MEC-AD reactor) that were operated for 131 d in continuous mode at different OLRs (1.1, 1.7 and 2.9 $g_{COD}/(L \times d)$), was employed. The results from the fitting of particulate and soluble compounds (COD, carbon, and nitrogen) and the produced biogas, along with its methane content, showed that the obtained kinetics of the MEC-AD reactor improved significantly in comparison with the conventional AD reactor. In particular, the effect of the applied voltage indicated a predominant contribution to the biomass yields and the disintegration of complex particulates, resulting in a fourfold increase relative to the AD reactor. In addition, the first-order disintegration kinetics of other particulate substances and the substrates' Monod uptake kinetic rates were also improved, albeit to a lesser extent. In this context, the disintegration of complex particulates appeared to be the most sensitive parameter to changes, resulting in the highest variations of tCOD decomposition, which renders the applied potential a crucial factor for the elimination of the hydrolysis as the rate-limiting step of conventional AD systems. The optimization of the process operation as a function of the OLR, based on the extraction of the kinetic parameters from the ADM1, showed that in the case of the MEC-AD reactor, the highest divergence from the AD reactor in particulate and soluble COD content was obtained at an OLR of 4.14 $g_{COD}/(L \times d)$. Moreover, the

MEC-AD reactor performance and kinetic constants further improved as a function of an increased SRT, which is attributed to its increased biomass yields, which also became more apparent as a function of the increased OLR. Future research could be directed towards the development of a modified model that includes the integration of the bioelectrochemical interactions and redox reactions taking place on the electrodes, along with the existing AD biochemical processes, as well as the development of a qualitative prediction of additional microbial consortia, which facilitate the bioelectrochemical interactions. The results can serve as a practical imprint of the potential that the MEC-AD system operating parameters have on improving and accelerating WAS treatment.

Author Contributions: Conceptualization, G.K. and G.A.; data curation, G.K., A.T. and G.A.; formal analysis, G.K., A.T. and G.A.; funding acquisition, G.K.; investigation, G.K. and G.A.; methodology, G.K. and G.A.; project administration, G.L.; resources, G.L.; software, G.A.; supervision, G.L.; validation, G.K., A.T. and G.A.; visualization, G.K.; writing—original draft, G.K.; writing—review and editing, A.T. and G.L. All authors have read and agreed to the published version of the manuscript.

Funding: The research work was supported by the Hellenic Foundation for Research and Innovation (HFRI) under the 3rd Call for HFRI PhD Fellowships (Fellowship Number: 5675).

Data Availability Statement: The data presented in this study are available on request from the corresponding author.

Conflicts of Interest: The authors declare no conflict of interest. The funders had no role in the design of the study; in the collection, analyses, or interpretation of data; in the writing of the manuscript; or in the decision to publish the results.

References

1. Stamatelatou, K.; Antonopoulou, G.; Lyberatos, G. *Production of Biogas via Anaerobic Digestion*; Woodhead Publishing Limited: Sawston, UK, 2011; Volume 1895.
2. Ferrentino, R.; Langone, M.; Fiori, L.; Andreottola, G. Full-Scale Sewage Sludge Reduction Technologies: A Review with a Focus on Energy Consumption. *Water* **2023**, *15*, 615. [CrossRef]
3. Domini, M.; Bertanza, G.; Vahidzadeh, R.; Pedrazzani, R. Sewage Sludge Quality and Management for Circular Economy Opportunities in Lombardy. *Appl. Sci.* **2022**, *12*, 10391. [CrossRef]
4. Joicy, A.; Seo, H.; Lee, M.E.; Kim, D.H.; Cho, S.K.; Ahn, Y. Enhanced methane production using pretreated sludge in MEC-AD system: Performance, microbial activity, and implications at different applied voltages. *Int. J. Hydrogen Energy* **2022**, *47*, 40731–40741. [CrossRef]
5. Wang, X.T.; Zhang, Y.F.; Wang, B.; Wang, S.; Xing, X.; Xu, X.J.; Liu, W.Z.; Ren, N.Q.; Lee, D.J.; Chen, C. Enhancement of methane production from waste activated sludge using hybrid microbial electrolysis cells-anaerobic digestion (MEC-AD) process—A review. *Bioresour. Technol.* **2022**, *346*, 126641. [CrossRef]
6. Appels, L.; Baeyens, J.; Degrève, J.; Dewil, R. Principles and potential of the anaerobic digestion of waste-activated sludge. *Prog. Energy Combust. Sci.* **2008**, *34*, 755–781. [CrossRef]
7. Zhen, G.; Lu, X.; Kato, H.; Zhao, Y.; Li, Y.Y. Overview of pretreatment strategies for enhancing sewage sludge disintegration and subsequent anaerobic digestion: Current advances, full-scale application and future perspectives. *Renew. Sustain. Energy Rev.* **2017**, *69*, 559–577. [CrossRef]
8. Gonzalez, A.; Hendriks, A.T.W.M.; van Lier, J.B.; de Kreuk, M. Pre-treatments to enhance the biodegradability of waste activated sludge: Elucidating the rate limiting step. *Biotechnol. Adv.* **2018**, *36*, 1434–1469. [CrossRef]
9. Huang, X.; Yun, S.; Zhu, J.; Du, T.; Zhang, C.; Li, X. Mesophilic anaerobic co-digestion of aloe peel waste with dairy manure in the batch digester: Focusing on mixing ratios and digestate stability. *Bioresour. Technol.* **2016**, *218*, 62–68. [CrossRef]
10. Wang, Z.; Yun, S.; Xu, H.; Wang, C.; Zhang, Y.; Chen, J.; Jia, B. Mesophilic anaerobic co-digestion of acorn slag waste with dairy manure in a batch digester: Focusing on mixing ratios and bio-based carbon accelerants. *Bioresour. Technol.* **2019**, *286*, 121394. [CrossRef]
11. Xu, H.; Yun, S.; Wang, C.; Wang, Z.; Han, F.; Jia, B.; Chen, J.; Li, B. Improving performance and phosphorus content of anaerobic co-digestion of dairy manure with aloe peel waste using vermiculite. *Bioresour. Technol.* **2020**, *301*, 122753. [CrossRef]
12. Jia, B.; Yun, S.; Shi, J.; Han, F.; Wang, Z.; Chen, J.; Abbas, Y.; Xu, H.; Wang, K.; Xing, T. Enhanced anaerobic mono- and co-digestion under mesophilic condition: Focusing on the magnetic field and Ti-sphere core–shell structured additives. *Bioresour. Technol.* **2020**, *310*, 123450. [CrossRef] [PubMed]
13. Gong, Z.; Yu, H.; Zhang, J.; Li, F.; Song, H. Microbial electro-fermentation for synthesis of chemicals and biofuels driven by bi-directional extracellular electron transfer. *Synth. Syst. Biotechnol.* **2020**, *5*, 304–313. [CrossRef] [PubMed]

14. Huang, Q.; Liu, Y.; Dhar, B.R. A critical review of microbial electrolysis cells coupled with anaerobic digester for enhanced biomethane recovery from high-strength feedstocks. *Crit. Rev. Environ. Sci. Technol.* **2022**, *52*, 50–89. [CrossRef]
15. Sun, R.; Zhou, A.; Jia, J.; Liang, Q.; Liu, Q.; Xing, D.; Ren, N. Characterization of methane production and microbial community shifts during waste activated sludge degradation in microbial electrolysis cells. *Bioresour. Technol.* **2015**, *175*, 68–74. [CrossRef]
16. Ding, A.; Yang, Y.; Sun, G.; Wu, D. Impact of applied voltage on methane generation and microbial activities in an anaerobic microbial electrolysis cell (MEC). *Chem. Eng. J.* **2015**, *283*, 260–265. [CrossRef]
17. Xing, T.; Yun, S.; Li, B.; Wang, K.; Chen, J.; Jia, B.; Ke, T.; An, J. Coconut-shell-derived bio-based carbon enhanced microbial electrolysis cells for upgrading anaerobic co-digestion of cow manure and aloe peel waste. *Bioresour. Technol.* **2021**, *338*, 125520. [CrossRef]
18. Liu, J.; Yun, S.; Wang, K.; Liu, L.; An, J.; Ke, T.; Gao, Y.; Zhang, X. Enhanced methane production in microbial electrolysis cell coupled anaerobic digestion system with MXene accelerants. *Bioresour. Technol.* **2023**, *380*, 129089. [CrossRef]
19. Chen, Y.; Yu, B.; Yin, C.; Zhang, C.; Dai, X.; Yuan, H.; Zhu, N. Biostimulation by direct voltage to enhance anaerobic digestion of waste activated sludge. *RSC Adv.* **2016**, *6*, 1581–1588. [CrossRef]
20. Ge, Y.; Tao, J.; Wang, Z.; Chen, C.; Mu, L.; Ruan, H.; Yon, Y.R.; Su, H.; Yan, B.; Chen, G. Modification of anaerobic digestion model No.1 with Machine learning models towards applicable and accurate simulation of biomass anaerobic digestion. *Chem. Eng. J.* **2023**, *454*, 140369. [CrossRef]
21. Ozgun, H. Anaerobic Digestion Model No. 1 (ADM1) for mathematical modeling of full-scale sludge digester performance in a municipal wastewater treatment plant. *Biodegradation* **2019**, *30*, 27–36. [CrossRef]
22. Weinrich, S.; Nelles, M. Systematic simplification of the Anaerobic Digestion Model No. 1 (ADM1)—Model development and stoichiometric analysis. *Bioresour. Technol.* **2021**, *333*, 125124. [CrossRef] [PubMed]
23. Parker, W.J. Application of the ADM1 model to advanced anaerobic digestion. *Bioresour. Technol.* **2005**, *96*, 1832–1842. [CrossRef] [PubMed]
24. Batstone, D.J.; Keller, J. Industrial applications of the IWA anaerobic digestion model No. 1 (ADM1). *Water Sci. Technol.* **2003**, *47*, 199–206. [CrossRef] [PubMed]
25. Emebu, S.; Pecha, J.; Janáčová, D. Review on anaerobic digestion models: Model classification & elaboration of process phenomena. *Renew. Sustain. Energy Rev.* **2022**, *160*, 112288. [CrossRef]
26. Mo, R.; Guo, W.; Batstone, D.; Makinia, J.; Li, Y. Modifications to the anaerobic digestion model no. 1 (ADM1) for enhanced understanding and application of the anaerobic treatment processes—A comprehensive review. *Water Res.* **2023**, *244*, 120504. [CrossRef]
27. Wu, D.; Li, L.; Zhao, X.; Peng, Y.; Yang, P.; Peng, X. Anaerobic digestion: A review on process monitoring. *Renew. Sustain. Energy Rev.* **2019**, *103*, 1–12. [CrossRef]
28. Zou, L.; Wang, C.; Zhao, X.; Wu, K.; Liang, C.; Yin, F.; Yang, B.; Liu, J.; Yang, H.; Zhang, W. Enhanced anaerobic digestion of swine manure via a coupled microbial electrolysis cell. *Bioresour. Technol.* **2021**, *340*, 125619. [CrossRef]
29. Nguyen, V.T.; Ta, Q.T.H.; Nguyen, P.K.T. Artificial intelligence-based modeling and optimization of microbial electrolysis cell-assisted anaerobic digestion fed with alkaline-pretreated waste-activated sludge. *Biochem. Eng. J.* **2022**, *187*, 108670. [CrossRef]
30. Kanellos, G.; Tremouli, A.; Arvanitakis, G.; Lyberatos, G. Boosting methane production and raw waste activated sludge treatment in a microbial electrolysis cell-anaerobic digestion (MEC-AD) system: The effect of organic loading rate. *Bioelectrochemistry* **2024**, *155*, 108555. [CrossRef]
31. Feng, Q.; Song, Y.C.; Bae, B.U. Influence of applied voltage on the performance of bioelectrochemical anaerobic digestion of sewage sludge and planktonic microbial communities at ambient temperature. *Bioresour. Technol.* **2016**, *220*, 500–508. [CrossRef]
32. Liu, X.; Chen, Q.; Sun, D.; Wang, Y.; Dong, H.; Dang, Y.; Holmes, D.E. Applying potentials to conductive materials impairs High-loading anaerobic digestion performance by affecting direct interspecies electron transfer. *Bioresour. Technol.* **2019**, *297*, 122422. [CrossRef] [PubMed]
33. Choi, K.S.; Kondaveeti, S.; Min, B. Bioelectrochemical methane (CH4) production in anaerobic digestion at different supplemental voltages. *Bioresour. Technol.* **2017**, *245*, 826–832. [CrossRef] [PubMed]
34. Chen, X.; Xiao, B.; Tang, X.; Bian, C.; Liu, J.; Li, L. Microbial electrolysis cell simultaneously enhancing methanization and reducing hydrogen sulfide production in anaerobic digestion of sewage sludge. *Chemosphere* **2023**, *337*, 139445. [CrossRef] [PubMed]
35. Manjusha, C.; Beevi, B.S. Mathematical Modeling and Simulation of Anaerobic Digestion of Solid Waste. *Procedia Technol.* **2016**, *24*, 654–660. [CrossRef]
36. Henze, M.; Grady, C.P.L.; Gujer, W.; Marais, G.V.R.; Matsuo, T. A general model for single-sludge wastewater treatment systems. *Water Res.* **1987**, *21*, 505–515. [CrossRef]
37. Batstone, D.J.; Keller, J.; Angelidaki, I.; Kalyuzhny, S.V.; Pavlostathis, S.G.; Rozzi, A.; Sanders, W.T.M.; Siegrist, H.; Vavilin, V.A. Anaerobic digestion model No. 1 (ADM1). *Water Sci. Technol.* **2002**, *45*, 65–73. [CrossRef]
38. Tutorial, A.; Reichert, P. *Computer Program for the Identication and Simulation of Aquatic Systems*; Swiss Federal Institute for Environmental Science and Technology (EAWAG): Dubendorf, Switzerland, 1998.
39. Lee, S.H.; Kang, H.J.; Kim, Y.; Kim, N.K.; Park, H.D. Different contribution of exoelectrogens in methanogenesis via direct interspecies electron transfer (DIET) by the different substrate in continuous anaerobic bioreactor. *Bioresour. Technol.* **2022**, *364*, 128115. [CrossRef]

40. Yun, S.; Fang, W.; Du, T.; Hu, X.; Huang, X.; Li, X.; Zhang, C.; Lund, P.D. Use of bio-based carbon materials for improving biogas yield and digestate stability. *Energy* **2018**, *164*, 898–909. [CrossRef]
41. Gharbi, R.; Vidales, A.G.; Omanovic, S.; Tartakovsky, B. Mathematical model of a microbial electrosynthesis cell for the conversion of carbon dioxide into methane and acetate. *J. CO2 Util.* **2022**, *59*, 101956. [CrossRef]
42. Huang, Q.; Liu, Y.; Dhar, B.R. Boosting resilience of microbial electrolysis cell-assisted anaerobic digestion of blackwater with granular activated carbon amendment. *Bioresour. Technol.* **2023**, *381*, 129136. [CrossRef]
43. Sasaki, D.; Sasaki, K.; Watanabe, A.; Morita, M.; Matsumoto, N.; Igarashi, Y.; Ohmura, N. Operation of a cylindrical bioelectrochemical reactor containing carbon fiber fabric for efficient methane fermentation from thickened sewage sludge. *Bioresour. Technol.* **2013**, *129*, 366–373. [CrossRef] [PubMed]
44. Jiang, J.; He, S.; Kang, X.; Sun, Y.; Yuan, Z.; Xing, T.; Guo, Y.; Li, L. Effect of Organic Loading Rate and Temperature on the Anaerobic Digestion of Municipal Solid Waste: Process Performance and Energy Recovery. *Front. Energy Res.* **2020**, *8*, 1–10. [CrossRef]
45. Yu, J.; Kim, S.; Kwon, O.S. Effect of applied voltage and temperature on methane production and microbial community in microbial electrochemical anaerobic digestion systems treating swine manure. *J. Ind. Microbiol. Biotechnol.* **2019**, *46*, 911–923. [CrossRef] [PubMed]
46. De La Rubia, M.A.; Perez, M.; Romero, L.I.; Sales, D. Effect of solids retention time (SRT) on pilot scale anaerobic thermophilic sludge digestion. *Process Biochem.* **2006**, *41*, 79–86. [CrossRef]
47. Gerardi, M.H. (Ed.) Retention times. In *The Microbiology of Anaerobic Digesters*; John Wiley & Sons, Inc.: Hoboken, NJ, USA, 2003; pp. 87–88.
48. Zhang, C.; Yun, S.; Li, X.; Wang, Z.; Xu, H.; Du, T. Low-cost composited accelerants for anaerobic digestion of dairy manure: Focusing on methane yield, digestate utilization and energy evaluation. *Bioresour. Technol.* **2018**, *263*, 517–524. [CrossRef]
49. Yun, S.; Zhang, C.; Wang, Y.; Zhu, J.; Huang, X.; Du, T.; Li, X.; Wei, Y. Synergistic effects of Fe salts and composite additives on anaerobic digestion of dairy manure. *Int. Biodeterior. Biodegrad.* **2019**, *136*, 82–90. [CrossRef]